City Research Online

City, University of London Institutional Repository

Designing efficient grid structures considering structural imperfection sensitivity

Fengcheng Liu[a,b], Ruoqiang Feng[b]*, Konstantinos Daniel Tsavdaridis[a], Guirong Yan[c]

[a] School of Civil Engineering, University of Leeds, Woodhouse Lane, LS2 9JT, Leeds UK
[b] The Key Laboratory of Concrete and Prestressed Concrete Structures of Ministry of Education, Southeast University, Nanjing 211189, China
[c] Department of Civil, Architectural and Environmental Engineering, Missouri University of Science and Technology, 1401 N. Pine St., Rolla, MO, USA

Abstract: At the initial design stage of a grid structure, shape optimisation is an effective way to find the optimal structural form. However, most of the shape optimisation methods do not take into consideration the imperfections, thus the actual buckling load capacity of the optimised structure is usually low. In this paper, an improved shape optimisation method is proposed, one that is considering the effect of structural imperfection sensitivity. In this method, the bending strain energy ratio is taken as a constraint, and when the total strain energy decreases, yet there is a certain proportion of bending strain energy in the structure. Consequently, the resulted shape is not sensitive to the initial geometry imperfection, and therefore, an efficient structure with higher buckling load capacity and low imperfection sensitivity is obtained. In order to evaluate the redundancy performance of the optimised structure, an index called structural overall redundancy, based on damage model is proposed herein. The damage model is simulated by removing a key rod of the structure. The results demonstrate that the overall redundancy of the structure obtained by the proposed method is higher than that obtained by the traditional method, thus an optimal design of a grid structure is obtained.

Keywords: *space grid structure; shape optimisation; imperfection sensitivity; bending strain energy; redundancy*

1. Introduction

In recent years, grid structures have become popular structural typologies thanks to their splendid visual effects and the capacity to cover large spaces with an uninterrupted span, see Fig. 1 [1]. They are widely used in a variety of building types, such as exhibition pavilions, stadiums, assembly halls and protective shelters [2]. People often marvel at the lightness of the structure and the fluidity of the lines. However, why are grid structures inherently beautiful? According to Malek and Willians [3], the aesthetics come with their superior structural efficiency since fewer materials are needed to resist such high loads. However, it is not an easy task for engineers to determinate the final optimal shape that respects architectural requirements and is structurally efficient at the same time. For this reason, the architectural aspects should always be treated together with the structural ones in the initial design phase of a grid structure.

For this reason, shape optimisation based on the structural performance is usually employed to the form-finding of grid shell structures. After years of research, many form-finding techniques have been developed such as the force density method, dynamic relaxation, updated reference strategy, and the particle-spring system method. Feng et al. [4],[5] studied the shape optimisation of cable-braced free-

---

form grid structures with the aim of reducing structural strain energy. Structural shape optimisation was realised by adjusting the generatrix and directrix rather than optimising the whole surface, as shown in Fig. 2, which improved the optimisation efficiency and resulted high engineering practical value. Winslow [6] proposed a novel algorithm to simulate the entire optimisation process of grid structures based on a traditional genetic algorithm (GA).

At a wider scope, Hawdon-Earl and Tsavdaridis [7] developed a standard and robust methodology for RC shell design for a complex site shape. The methodology uses Oasys GSA and Abaqus which allow both form-finding analysis and dimensioning to be conducted. The roof of Akrotiri, an archaeological site in Santorini island, Greece, was designed by this method and proved its applicability. Bochenek [8] studied the optimization of structures against instability, and the nonlinear behaviour of designed elements is considered. According to his research, different optimization designs can be obtained by including nonlinear structural behavior in the representation of optimization problems compared with traditional methods.Cui and Yan [9],[10] proposed many advanced structural morphosis techniques, such as the extended evolutionary structural optimisation method and the height adjusting method. With these methods, different architectural forms were obtained by changing different kinds of design parameters such as constraints or space conditions according to the designer's needs. All of the architectural form achieved by the above two methods can keep the structure in a mostly uniform axial-stress state and with the bending moment controlled. The shortcoming of the methods is that they did not consider the effect of the geometry imperfection on structural mechanical performance. Maggie et al. [11],[12] proposed a two-stage optimisation algorithm based on GA. Then, Kociecki and Adeli [13] extended the algorithm to shape optimization of the structures, which was performed simultaneously with size and topology optimization, and a free-form surface grid roof (Ottawa Railway Station) was studied by using the algorithm that resulted in a lightweight structure. Ding et al. [14] presented a node-shifting method for shape optimisation of reticulated spatial structures to enhance their stiffness. With the constraint of volume, jagged surfaces were automatically smoothed during the volume adjustment process, thus no extra smoothing procedure is required. The method was suitable for many types of single-layer grid structures including those with cantilevered parts. Liu et al. [15] proposed a modified double-control form-finding (MDFF) method for suspendomes considering the construction process and the friction of cable–strut joints. The incremental equilibrium equation is built to include geometric nonlinearity based on the total Lagrangian increment formulation. The results showed that the proposed method can provide more accurate nodal coordinates and cable forces of the initial geometry state. The nonlinear analysis and the optimum design of cable domes are studied by Yuan et al [16]. They considered two optimal variables, including prestress level and cross stress, respectively. The numerical results showed the accuracy and validity of the nonlinear analysis model and the optimum algorithms, which also indicated that their work is very useful for understanding the behaviour of cable domes.

It is well known that geometrical imperfection may cause a significant reduction in the buckling load capacity of shell structures. The optimisation for the buckling load capacity of shell structures has been investigated by Rritinger [17], Ohsaki [18], and Ohuchi [19]. Ohsaki [20] summarized the existing methods of design sensitivity analysis and optimization of elastic conservative finite-dimensional systems with respect to nonlinear buckling behavior and presented a new optimization results of flexible truss. It is worth to note that the buckling load capacity of the single-layer grid structure is also greatly influenced by the initial geometric imperfection. Sometimes even a small geometric imperfection can lead to a significant reduction in buckling load capacity.

In general, during shape optimisation of a single-layer grid structure, the structural total strain energy is usually set as the objective function. Rational structural shapes with high buckling load capacity are obtained by minimising the total strain energy. After the optimisation, the axial strain energy is dominated and there is little bending strain energy in the structure. Since the structure is dominated by axial compression, the imperfection sensitivity is gradually enhanced. However, if the structure is dominated by bending strain energy, the structure will be insensitive to geometric imperfection. In this case, the total strain energy will be large and the buckling load capacity of the structure will not be too high. Consequently, it is important to understand how to determine the relationship between the total strain energy and the bending strain energy. In the method proposed in this paper, while reducing the total strain energy, a certain proportion of bending strain energy in the structure is ensured. With this way, a rational shape with higher buckling load capacity and lower imperfection sensitivity can be obtained.

In the literature, researchers have tried to minimise the influence of the geometrical imperfection on the buckling load of the single-layer grid structure. However, the subject of the presented work is to demonstrate how to find a better shape of a single-layer grid structure which has both higher buckling load capacity and lower imperfection sensitivity. This can be achieved by adding the ratio of bending strain energy as another constraint based on the traditional shape optimisation method, in order to control the bending strain energy of a grid structure and reduce the structural imperfection sensitivity. In addition, with respect to the obtained shape based on the improved optimisation scheme, the structural redundancy performance is investigated.

2. Method of shape optimisation

2.1. Definition of imperfection sensitivity

The imperfection sensitivity is expressed as follows.

$$= \left| \frac{P_d \quad P_i}{P_i} \right| \cdot 100\% \tag{1}$$

Where P_d is the buckling load of the structure considering initial geometric imperfection; P_i is the buckling load of intact structure; the larger the greater influence of initial geometric imperfection on the buckling load of the structure and the more sensitive the structure is. In this paper, the imperfection was implemented according to the first-order eigenvalue buckling mode and the maximum value is 1/300 of the structural span, which meets the requirements of technical specification for space frame structures [21].

2.2. Traditional method of shape optimisation

The traditional method of shape optimisation, which minimises the total strain energy, can be expressed as follows.

Objective function $\quad C(z) = \frac{1}{2} U^T K U \qquad Min \tag{2}$

$$\text{Subject to} \qquad \dfrac{B}{400}$$

$$_{max} \quad 345MPa$$

Where C is the total strain energy, K is the stiffness matrix, U is the nodal displacement vector, z is the nodal z-coordinate. B is the short span of the structure,   is the maximum nodal displacement and

$_{max}$ is the maximum stress of the tubes.

After the optimisation, the buckling load capacity of the intact structure obtained by traditional method will become very high, but once the initial geometric imperfection is applied, the buckling load capacity of the structure will decrease significantly. The optimised structure is extremely sensitive to initial geometric imperfection; therefore, the consequence is that the actual buckling load capacity of the optimised is not high. The reason for this is that the traditional optimisation method does not consider the influence of initial geometrical imperfection and then the effectiveness of this method is greatly reduced. Finally, the traditional method cannot obtain the structural shape with high buckling load capacity once the initial geometric imperfection is applied.

2.3. Improved method of shape optimisation

In order to consider the influence of structural imperfection sensitivity in the process of shape optimisation, the bending strain energy ratio is proposed and set as another constraint in the improved method. In this paper, the bending strain energy ratio is defined as $R = C_2 / C$, where C is the total strain energy; C_2 is the bending strain energy that is expressed in equation (3).

$$C_2 = \frac{1}{2} U_z^{\,T} K_b U_z \tag{3}$$

Where K_b is the bending stiffness matrix; U_z is the out-of-plane nodal displacement vector. The difference between total strain energy and bending strain energy is the axial strain energy, while the torsional strain energy is neglected.

Taking the bending strain energy ratio as another constraint in the improved method, the bending strain energy inside the structure can be well controlled. It is ensured that the bending strain energy will not be too small while the total strain energy decreases. By this way, it can not only effectively improve the structural buckling load, but also reduce the sensitivity of the structure to the initial geometric imperfection, so as to obtain a better structural shape than the traditional optimisation method. However, in the improved method, the bending strain energy ratio have to be obtained by the designer's experience. In this paper, the traditional method of shape optimisation is implemented through the OptiStruct solver in HyperWorks software. It can be used to solve efficiently optimisation problems with millions of design variables or constraints. Nevertheless, the shortcoming of the software is that it cannot consider the bending strain energy. Therefore, the improved method is realised in the programming language MATLAB. The program of total strain energy and bending strain energy of the structure are compiled in MATLAB, and the genetic algorithm (GA) is chosen as the optimisation algorithm. The MATLAB GA toolbox was used and the objective function is the total strain energy which representing the fitness; the constraint are the maximum nodal displacement, the maximum stress of the tubes and the bending strain energy ratio. In this paper, the population type is double vector, the population size is 200, roulette is chosen as the selection method, the crossover fraction is 0.8, the stall generations is set to 50 and the

max generations is 1000. The initial range is changed due to the specified issues, and other parameters keep the default values.

3. Case studies of shape optimisation

3.1. Case 1--- a geodesic dome

A geodesic dome is a hemispherical lattice-shell based on a geodesic polyhedron, originally invented by R. Buckminster Fuller in 1954 [22], have been used for a wide range of purposes including temporary exposition structures and housing. The dome is very light but can withstand heavy loads. In order to reduce time consumption, this paper selects a part of the dome with the span of 5m and the height of

1m, as shown in Fig. 3(a). The rod is the steel pipe of $70 \cdot 3$, and the elastic modulus is $2.0 \cdot 10^5 MPa$.

The concentrated load is applied on each node as uniformly distributed load, including the rod weight, the finishing materials and the live load of 500 N/m^2. The surrounding supports are hinged and the z-direction coordinates of the internal nodes are set as design variables, as shown in Fig. 3(b).

3.1.1 Results of traditional method

Firstly, the traditional method is used to optimise the shape based on HyperWorks' Optistruct solver without considering the effects of structural initial geometry imperfection. As shown in Table. 1, after 40 iterations, the shape with the smallest total strain energy, was obtained which was generally considered to be the best structural form. A structural form is extracted every 5 iterations to study the variation of the buckling load capacity of various structural forms in the optimisation process with or without considering the initial geometric imperfection, and so as their changes in imperfection sensitivity. The comparison results of various typical structural forms are shown in the Table. 1. It can be seen that as the optimisation proceeds, the total strain energy and the bending strain energy ratio are both reduced, their variation curves are shown in Fig. 4 and Fig. 5. Finally, the axial strain energy is dominated in the structure, which will inevitably lead to an increase of the structural imperfection sensitivity. Fig. 6 indicates that as the optimisation proceeds the imperfection sensitivity of the structure increases, and the final structural form has the highest imperfection sensitivity. In this case, with regards to the structural buckling load capacity, the final shape has the highest buckling load capacity when does not consider the imperfection sensitivity; it has increased 9.8% compared to the initial shape. However, it cannot be ignored that the effect of geometric imperfection on its buckling load capacity is also gradually increasing, which has increased to 25.3%. Fig. 7 shows the variation of structural buckling load capacity during optimisation. It can be clearly seen that the buckling load capacity of the intact structure is always increasing and the final shape has the highest buckling load capacity. Nevertheless, once the geometric imperfection is considered, the buckling load capacity decreased significantly and the optimum shape with highest buckling load capacity appeared in the middle steps instead of the final step. In this case study, it is the 20th step in which the structural shape with the highest buckling load capacity appeared. Then, a preliminary conclusion can be drawn, such that the buckling load capacity of the intact structure is very high without considering the initial geometric imperfection. However, its imperfection sensitivity is also very high, which will lead to a significant decrease in the buckling load capacity when imperfection is applied. Therefore, it is impossible to obtain the best structural form using the traditional method.

According to the research conducted by the authors of this paper, the optimised structure has high imperfection sensitivity as the bending strain energy found inside the structure is too small after the

optimisation. In order to prevent this from happening, the solution is to adjust the ratio of bending strain energy inside the structure so as to reduce the imperfection sensitivity while ensuring the increase of structural buckling load capacity.

3.1.2 Results of the improved method

In the previous section, it was preliminary concluded, that if the internal bending strain energy of the structure is too small, it will lead to an increased imperfection sensitivity of the structure, which will eventually lead to a significant drop in the structural buckling load capacity. If the total strain energy of the structure is then reduced while ensuring that the internal bending strain energy of the structure does not become too small, a structural form with low imperfection sensitivity could be potentially obtained. Based on this approach, an improved shape optimisation method is proposed.

The improved method is implemented by MATLAB programming. The genetic algorithm (GA) is applied as an optimisation algorithm; z-coordinates of the internal nodes are chosen as design variables and the bending strain energy ratio is set as the constraint. It is worth noting that the bending strain energy ratio is obtained based on designer's experience. After the optimisation, five different shapes according to different constraints are obtained, as shown in Table 2. Model 1 is the initial shape and model 2 is obtained by the traditional method that does not consider the imperfection. Model 3-6 are achieved by the improved method considering the effect of imperfection.

It can be seen from Table 2 that the structure obtained by the traditional method has a lowest bending strain energy ratio of 0.0049, which is the basis for the changing of bending strain energy ratio in model 3-6. Model 3-6 are the results after increasing the ratio of bending strain energy. Evidently, when the bending strain energy ratio is increased, the imperfection sensitivity of the structure decreases significantly. Therefore, the structural buckling load capacity only slightly decreases when the initial imperfection is applied. It should be noted that with the increase of bending strain energy ratio, the total strain energy is also increased to some extent. As a result, the buckling load capacity of the intact structure of model 3-6 is not as high as that of model 2. However, it is worth noting that due to the low imperfection sensitivity, the buckling load capacity of model 3-5 after considering the geometric imperfection is higher than that of model 2, which illustrates the effectiveness of the improved optimisation method. Therefore, with the improved method, a better shape with higher buckling load capacity and lower imperfection sensitivity is achieved. In model 6, since the bending strain energy ratio increased too much and so does the total strain energy. Consequently, the buckling load capacity of the intact structure becomes very low. Although the imperfection sensitivity is very low, it is still impossible to obtain a structural form with a higher buckling load capacity after applying the geometric imperfection. It indicates that the selection of bending strain energy ratio is very important. However, at present, the value of bending strain energy ratio has to be determined depending on the designer's experience.

Fig. 8 shows the load-displacement curves of different models. Model 2 which is obtained by the traditional method has higher buckling load capacity when does not consider the geometric imperfection, as shown in Fig. 8(a). However, once the initial geometric imperfection is applied, the buckling load capacity of model 2 is no longer the highest. It is model 3 which has the highest buckling load capacity because of its low imperfection sensitivity and the relatively high buckling load capacity of its intact structure. Fig. 9 is the iterative curve of model 3. The total strain energy decreases rapidly in early stage. Then there are some fluctuations, and it tends to be stable in the later period of optimisation.

3.2. Case 2--- a free-form single-layer grid structure

In the previous section, a geodesic dome that belongs to the traditional analytical surface grid structure was studied. In this section, in order to verify the applicability of the improved method, a triangular free-form single-layer grid structure with four edges articulated is examined. As shown in Fig. 10, the initial shape is defined as a free-form surface of 21m in span and 2.5m in height (the rise). The structural parameters are the same as the geodesic dome described in the previous section. The location of nodes 9-17 and nodes 77-85 is shown in Fig. 10a.

3.2.1 Results of HyperWorks

Using the Optistruct solver, the optimised shape with minimum total strain energy is obtained after 33 iterations. Fig. 11 shows the z-coordinate movements by the optimisations of nodes 9-17. The cross-section has been arched upward, the structure is mainly subjected to axial force, and the total strain energy has become very small. The variation of structural strain energy in optimisation process is shown in Fig. 12. It can be seen that as optimisation proceeds, the structural strain energy decreases rapidly. The total strain energy, axial strain energy, and bending strain energy are reduced to 40%, 47%, and 1% of the initial structure, respectively. Among them, the bending strain energy decreases the fastest. Finally, the axial strain energy is dominant in the structure.

Considering both geometric and material nonlinearity, the full-process analysis of all of 33 models are completed. The variation of buckling load capacity of the structure during the process of optimisation is obtained, as shown in Fig. 13. Combining with Table 3, the buckling load capacity of the intact structure has been greatly improved when the optimisation is terminated at step 33, which is about three times of the initial structure. At the same time, according to the consistent mode imperfection method, the least order mode of eigenvalue buckling mode is taken as the corresponding imperfection distribution mode, and the buckling load capacity of the structure is decreased after the initial geometric imperfection is applied. It should be noted that when the initial geometric imperfection is considered, the structural form with the highest buckling load capacity does not appear in the final step but the 7th step in this case study. The structural buckling load capacity of step 7 is 1.48 times the 33 step and 1.6 times of the initial state when the imperfection is applied. It suggests that the traditional optimisation method cannot obtain the structural form with high buckling load capacity after the initial geometric imperfection is applied.

Fig. 14 shows the variation of structural imperfection sensitivity along with the iterations. It can be seen that as the optimisation proceeds, the structural imperfection sensitivity increases significantly. In the later stage of optimisation, the imperfection sensitivity is obviously greater than that in the early stage of optimisation, reaching more than 60%. Therefore, when the initial geometric imperfection is applied, the structural buckling load capacity decreased by 60%, which critically affects the optimisation effect and reduces the effectiveness of traditional optimisation method.

3.2.2 Results of MATLAB

With the improved method, six different shapes of the free-form grid structure according to different

constraints are obtained. The contrast of shapes is shown in Fig. 15, and model 1 is the initial shape that is represented by the dotted line, model 2 is the shape obtained through the traditional method, model 3-7 are shapes obtained by the improved method. The comparison of the result data is shown in Table 4.

Comparing the above seven models, the maximum buckling load capacity of the intact structure occurs in model 2, but its imperfection sensitivity has reached to 51.6%, which indicates that the structural shape obtained by the traditional method is especially sensitive to geometrical imperfection. In model 3, the value of bending strain energy ratio is doubled, and the total strain energy of the structure remains the same. As the bending strain energy ratio increased, the imperfection sensitivity and buckling load capacity of the intact structure is decreased. However, the buckling load capacity considering the imperfection in model 3 is still lower than in model 2, which suggests that the value of bending strain energy ratio in model 3 is not reasonable. In model 4, the value of bending strain energy ratio is expanded by 1.6 times, and the total strain energy is expanded appropriately. In this case, the buckling load capacity of the intact structure is decreased again and the imperfection sensitivity has fallen by 48.9%. On the other hand, the buckling load capacity considering the imperfection in model 4 is 7% higher than that in model 2, which suggests that the structural shape in model 4 is better than that in model 2.

In model 5, the bending strain energy ratio is expanded by three times. As shown in Table 4, the imperfection sensitivity and the buckling load capacity of the intact structure continues to decrease and an ideal structural shape occurs. The buckling load capacity considering imperfection in model 5 is 17% higher than that in model 2. With the increase of total strain energy and bending strain energy ratio of the structure, an optimum structural shape with higher buckling load capacity and lower imperfect sensitivity is obtained in model 6 when the imperfection is considered. In this case, the imperfection sensitivity has reduced to 6% significantly, and the buckling load capacity considering imperfection is 48% higher than that in model 2.

As the bending strain energy continues to increase, the total strain energy will increase at the same time. The consequence is that the buckling load capacity of the intact structure will continue to decrease.

For this example, the suitable bending strain energy ratio is 0.03 and the total strain energy is 374.98J. It is known from table 4, that the buckling load capacity of intact structure tends to increase along with the decrease of total strain energy, while the imperfection sensitivity will be decreased along with the increase of the bending strain energy ratio.

Load-displacement curves of different models are shown in Fig. 16. Obviously, if the initial imperfection is not applied, the buckling load capacity of each model is much higher than that of the model 1 and the buckling load capacity of model 2 is the highest. However, once the imperfection is considered, as shown in Fig. 16(b), the buckling load capacity of model 2 is no longer the highest; the highest buckling load capacity occurs in model 6 with 1.48 times higher than that of model 2.

The coordinate changes of nodes 77-85 in each model are shown in Fig. 17. Compared with the initial shape, all of the models are upward convex. This is due to the decrease in structural strain energy resulting in a change in the shape of the structure. Being upward convex is to make the structure dominated by the axial force. On the other hand, the left side of model 6 is similar to the initial shape; only on the right side, the convex, is more obvious. That is because the bending strain energy ratio is limited and the amplitude of the convex of the structure is constrained accordingly. Fig. 18 is the iterative curve of model 6. It shows that in the early stage of the optimisation, the total strain energy decreases rapidly. In the middle process, there are some fluctuations, and in the later period of

optimisation, it tends to be stable. Finally, after 237 iterations, the optimisation terminates and an ideal shape is obtained.

4. Redundancy evaluation of the optimised structure

4.1. Overall redundancy of the structure

The need for structural safety under a variety of loading and accident conditions has focused attention on redundancy, ductility, and reliability of structural systems. From this point of view, in order to evaluate the redundancy performance of the optimised structure obtained by the improved method, an overall structural redundancy index R_e based on damage model is proposed in this paper.
The overall structural redundancy is defined as:

$$R_e = \frac{P_{per}}{P_{per} - P_{da}} \tag{4}$$

Where P_{da} is the ultimate strength of the damaged structure, P_{per} is the ultimate strength of the undamaged structure. In this paper, the damaged structure is simulated by removing a key member in a single-layer grid structure. Moreover, the key member is determined according to the structural component redundancy.

4.2. Component redundancy

According to Pandey [23], for a given structure and loading, the generalised redundancy is directly proportional to the insensitivity of structural elements, or inversely proportional to their response sensitivity under consideration.

$$Generalized\ redundancy \propto \frac{1}{response\ sensitivity} \tag{5}$$

On the bases of Pandey's study, the structural component redundancy was defined based on the sensitivity of structural strain response to the cross-sectional area of the rods.
Therefore, the structural component redundancy can be defined as:

$$component\ redundancy = \frac{V_i}{strain\ response} \tag{6}$$

In the space grid structure, due to the large number of the elements, the weighted average method is used to define the structural component redundancy.
Therefore, the redundancy of element i in grid structure can be defined as:

$$GRi = \frac{\sum_{j=1}^{ne}(\frac{V_j}{S_{ji}})}{V}, i = 1, 2, ... ne \tag{7}$$

Where V_j is the volume of element j, S_{ji} is the strain energy response sensitivity of the jth element for the cross-sectional area of the element i. For beam elements, S_{ji} is the maximum of bending strain energy, tensile strain energy, and shear strain energy, that is to say $S_{ji} = \max(\varepsilon_j^e / A^i)$. Moreover, ne is

the number of elements in grid structure; V is the total volume of the structure.

The derivation process is described in detail below. For elastic structures, after considering the design variables, the equilibrium equation can be expressed as

$$K(A_i)U(A_i) = F(A_i) \tag{8}$$

Where A_i is the cross-section area of the ith element.

The nodal displacement sensitivity depending on the element area A is obtained by deriving A on both sides of the upper formula, which can be expressed as

$$\partial U / \partial A^i = K^{-1}[\partial F / \partial A^i - (\partial K / \partial A^i)U] \tag{9}$$

Generally, the external load acting on the structure has nothing to do with the section area of the element, so the upper formula can be changed to

$$\partial U / \partial A^i = -K^{-1}(\partial K / \partial A^i)U \tag{10}$$

In the formula, the integral stiffness matrix K of the structure is integrated from the element stiffness matrix k_i^e. Moreover, the displacement sensitivity of the structural stiffness matrix can be written as

$$\partial K / \partial A^i = \sum_{i=1}^{ne} R_i^T (\partial k_i^e / \partial A^i)R_i \tag{11}$$

Then, according to the relationship between elemental strain and nodal displacement $\varepsilon_j^e = Bu_j^e$. The elemental strain sensitivity can be written as

$$\partial \varepsilon_j^e / \partial A^i = B(\partial u_j^e / \partial A^i) + (\partial B / \partial A^i)u_j^e \tag{12}$$

Where $\partial B / \partial A^i$ is the sensitivity of strain matrix to the cross-section area; $\partial u_j^e / \partial A^i$ is the sensitivity of the nodal displacement of node j to the cross-section area in the local coordinate system.

Since the strain matrix is independent of the elemental cross-section area, the upper formula can be rewritten to

$$\partial \varepsilon_j^e / \partial A^i = B(\partial u_j^e / \partial A^i) \tag{13}$$

Where $\partial u_j^e / \partial A^i = R_j(\partial U_j^e / \partial A^i)$ can obtain from formula (10). Finally, the maximum of bending strain energy, tensile strain energy and shear strain energy in formula (13) is chosen as the strain energy response sensitivity of the jth element. Then take it into formula (7) to get the component redundancy of element i in the grid structure. Both the component redundancy and the overall structural redundancy are obtained using the MATLAB code.

4.3. Verification of the redundancy evaluation method

The key of redundancy analysis method provided in this paper is how to determine the key rods. In this paper, the key member is determined according to the structural component redundancy, which was proposed by Pandey [23]. In addition, it is illustrated that the structural elements with low redundancies

are the key components of the structure by Hua [24]. In order to verify the correctness of the author's program, a 24-member dome used by Hua [24] was taken as an example in this paper, as shown in Fig.19. Structural parameters of the 24-member dome used in this paper are the same as in the literature. The redundancy of components under vertical load was shown in Table 5. It can be seen that the result obtained by the author is very similar with that in the literature. The error does not exceed 5%, which indicates that the redundancy evaluation method used in this paper is correct and feasible.

4.4. Redundancy evaluation of single-layer grid structure

In order to evaluate the overall redundancy performance of the structure, the free-form single-layer grid structure in the previous section is chosen as the computational model. Firstly, the key rods that will be removed later should be determined. According to the definition of component redundancy, the component redundancy of all the rods in model 2 and Model 6 are calculated, respectively. Then, the rods with less redundancy are chosen as the key rods, which will be removed when calculating overall redundancy of the structure, and then the overall redundancy of model 2 and model 6 are calculated, respectively.

In this paper, the first 10 rods with less component redundancy in model 6 are chosen as the structural key rods, as shown in Fig. 20. The location of the key rods is shown in Fig. 21 and the thickness of the lines indicate the magnitude of the component redundancy. For better comparison, the rods with the same number in model 2 will also be removed. Therefore, 10 groups as shown in Table 6 are obtained. As seen from the table, the first 10 rods with less redundancy in model 6 also have a relatively small component redundancy in Model 2. It is worth noting that only one key rod is removed from each group. By comparing the overall redundancy of these 10 groups, it can be concluded that the overall redundancy of model 6 is relatively high after the removal of the key rod, with only one exception. It suggests that the improved shape optimisation method can get a better shape which with high overall redundancy.

5 Conclusions

The resulted structure obtained by the traditional optimisition method is very sensitive to initial geometric imperfections due to the lower bending strain energy in the structure. Consequently, the actual buckling load capacity is low after the application of the initial imperfection. An improved optimisation method which takes the bending strain energy ratio as the constraint is presented in this paper. With this method, the total strain energy can be reduced while ensuring that the bending strain energy inside the structure does not become too small.

Two cases including an analytical surface grid structure and a free-form surface grid structure have been studied and the results indicate that the proposed method can effectively eliminate the adverse effects caused by the initial imperfection. With the improved method, a better structural shape with improved buckling load capacity and lower imperfection sensitivity is obtained. Then, the feasibility of the method is proved.

Furthermore, in order to evaluate the structural redundancy performance, an index called overall redundancy of the structure based on the damage model is proposed in this paper. The results show that the overall redundancy of the structure obtained by the improved method is higher than that obtained by the traditional method, which indicates that the improved method can obtain an efficient grid structure.

References

[1]   Schlaich J, Schober H. (2002). Design principles of glass roofs. Lightweight Structures in Civil Engineering Proceedings of the International Symposium, Warsaw, Poland. 24-28.

[2]   Iuorio, O., Homma, E. and Tsavdaridis, K.D. (2016) The Application of Free-Form Grid Shells as Protective Shelters in Archeological Sites. International Association for Shell and Spatial Structures Symposium (IASS 2016). 26-30 September, Tokyo, Japan.

[3]   Malek, S. and C. J. Williams (2017). "Reflections on the Structure, Mathematics and Aesthetics of Shell Structures." Nexus Network Journal 19(3): 555-563.

[4]   Feng Ruoqiang, Ge Jinming, Ye Jihong. (2013) Shape optimisation of free-form cable-braced grid shells. China Civil Engineering Journal, 46 (4): 64-70.

[5]   Feng Ruoqiang, Ge Jinming, Hu Lipeng, et al. (2015) Multi-objective shape optimisation of free-form cable-braced grid shells with B-spline method.China Civil Engineering Journal, 48(6):1-8.

[6]   Winslow P, Pellegrino S, Sharma S B. (2010). Multi-objective optimisation of free-form grid structures. Structural and multidisciplinary optimisation, 40(1-6): 257-269.

[7]   Hawdon-Earl, S. and Tsavdaridis, K.D. (2018). Form Finding and Dimensioning of Reinforced Concrete Shell Roof for Akrotiri (Santorini). Journal of the International Association for Shell and Spatial Structures (IASS).59(4), 198.

[8]   Bochenek B. (1997). Optimization of geometrically nonlinear stuctures with respect to both buckling and postbuckling constraints. Engineering Optimization, 29(1-4): 401-415.

[9]   Cui C, Yan H. (2006). An advanced structural morphosis technique Extended evolutionary structural optimisation method and its engineering applications. China Civil Engineering Journal, 39(10): 42-47.

[10] Cui C, Yan H. (2006). A morphosis technique for curved-surface structures of arbitrary geometries---Height adjusting method and its engineering applications. China Civil Engineering Journal, 12.

[11] Kociecki M, Adeli H. (2013). Two-phase genetic algorithm for size optimisation of free-form steel space-frame roof structures. Journal of Constructional Steel Research, 90: 283-296.

[12] Kociecki M, Adeli H. (2014). Two-phase genetic algorithm for topology optimisation of free-form steel space-frame roof structures with complex curvatures. Engineering Applications of Artificial Intelligence, 32: 218-227.

[13] Kociecki M, Adeli H. (2015). Shape optimization of free-form steel space-frame roof structures with complex geometries using evolutionary computing. Engineering Applications of Artificial Intelligence, 38: 168-182.

[14] Ding C, Seifi H, Dong S, et al. (2017). A new node-shifting method for shape optimisation of reticulated spatial structures. Engineering Structures, 152: 727-735.

[15] Liu H, Zhang W, Yuan H, et al. (2016). Modified double-control form-finding analysis for suspendomes considering the construction process and the friction of cable–strut joints. Engineering Structures, 120: 75-81.

[16] Yuan X F, Dong S U. (2002). Nonlinear analysis and optimum design of cable domes. Engineering Structures, 24(7): 965-977.

[17] Reitinger R, Ramm E. (1995). Buckling and imperfection sensitivity in the optimisation of shell structures. Thin-walled structures, 23(1-4): 159-177.

[18] Ohsaki M, Uetani K, Takeuchi M. (1998). Optimisation of imperfection-sensitive symmetric systems for specified maximum load factor. Computer methods in applied mechanics and engineering, 166(3-4): 349-362.

[19] Ohuchi S, Yamamoto K. (2016). Elasto-plastic Buckling Strength of Lattice Shells Shape-Optimized For Bending Strain Energy or Linear Buckling Load. Proceedings of IASS Annual Symposia. International Association for Shell and Spatial Structures (IASS), (2): 1-10.

[20] Ohsaki M. (2005). Design sensitivity analysis and optimization for nonlinear buckling of finite-dimensional elastic conservative structures[J]. Computer methods in applied mechanics and engineering, 194(30-33): 3331-3358.

[21] Technical specification for space frame structures (2010). Peking: China Building Industry Press, pp. 14-15.

[22] Fuller, R.B. (1954). Building Construction. Patent No. 2,682,235.

[23] Pandey P C, Barai S V. (1997). Structural Sensitivity as a Measure of Redundancy. Journal of Structural Engineering, 123(3): 360-364.

[24] Jing-Jing H, Ji-Hong YE. Redundancy of single-layer reticulated dome based on strain response sensitivity. Chinese Journal of Computational Mechanics, 2013, 30(6):783-776.

TABLES

Table 1 Comparison of results obtained by the traditional method

Step	Buckling load P_u (N)		Imperfection sensitivity (%)	Total strain energy C (J)	Bending strain energy ratio R	Total mass (kg)
	Intact structure	Considering imperfection				
0	2324.76	1864.36	19.804	291.59	0.00587	834.73
5	2426.96	1967.99	18.911	265.56	0.00567	840.90
10	2428.75	1882.90	22.475	247.36	0.00453	846.17
15	2434.08	1870.02	23.173	231.66	0.00444	850.63
20	2451.08	2282.94	6.860	217.94	0.00398	856.30
25	2460.51	1879.01	23.633	206.31	0.00393	861.56
30	2472.45	1887.56	23.656	196.01	0.00377	867.03
35	2523.91	2193.99	13.072	187.36	0.00362	872.40
40	2532.36	1891.33	25.314	181.77	0.00306	877.46

Table 2 Comparison of results obtained by the improved method

Model number	Buckling load P_u (N)		Imperfection sensitivity (%)	Total strain energy C (J)	Bending strain energy ratio R	Total mass (kg)
	Intact structure	Considering imperfection				
1	2324.76	1864.36	19.804	291.59	0.0058	834.73
2	2516.46	1999.36	20.549	184.03	0.0049	875.64
3	2409.59	2305.84	4.306	190.07	0.0067	871.49
4	2256.45	2281.37	1.104	199.98	0.0112	868.14

| 5 | 2323.07 | 2170.99 | 6.547 | 204.97 | 0.0132 | 867.13 |
| 6 | 1932.09 | 1857.48 | 3.862 | 206.11 | 0.0161 | 870.68 |

Table 3 Data comparison of typical iterative step results

| Step | Buckling load P_u (N) | | Imperfection sensitivity (%) | Total strain energy C(J) | Bending strain energy C_2(J) | Bending strain energy ratio R | Total mass (kg) |
	Intact structure	Considering imperfection					
0	4140.69	4520.6	9.17	953.65	170.28	0.179	7448.57
2	5300.22	5522.7	4.19	712.96	66.47	0.093	7451.18
7	9024.34	7287.01	19.25	515.30	14.30	0.028	7450.88
8	9314.41	7191.03	22.79	501.60	9.94	0.02	7451.48
18	11714.2	5517.05	52.91	413.38	4.18	0.01	7458.29
29	12928.5	4799.91	62.87	379.17	1.49	0.004	7464.12
33	12356.7	4897.75	60.36	372.75	1.82	0.005	7469.17

Table 4 The optimisation results

| Model number | Buckling load P_u (N) | | Imperfection sensitivity (%) | Total strain energy C(J) | Bending strain energy ratio R | Total mass (kg) |
	Intact structure	Considering imperfection				
1	4140.69	4520.60	9.175	953.65	0.179	7448.57
2	13205.80	6390.12	51.611	321.41	0.007	7472.14
3	12344.60	6279.76	49.129	321.39	0.014	7473.26
4	9118.37	6829.23	25.105	364.98	0.018	7463.24
5	8763.36	7459.05	14.884	372.73	0.028	7465.89
6	10076.10	9471.19	6.003	374.98	0.030	7467.66
7	8186.90	7831.96	4.335	400.99	0.045	7460.33

Table 5 Redundancy of components under vertical load

| Rod No. | Redundancy | | Rod No. | Redundancy | | Rod No. | Redundancy | | Rod No. | Redundancy | |
	This paper	Literature		This paper	Literature		This paper	Literature		This paper	Literature
1	26.8	28.2	7	42.9	44.4	13	22.8	22.6	19	22.8	22.6
2	26.8	28.2	8	42.9	44.4	14	22.8	22.6	20	22.8	22.6
3	26.8	28.2	9	42.9	44.4	15	22.8	22.6	21	22.8	22.6
4	26.8	28.2	10	42.9	44.4	16	22.8	22.6	22	22.8	22.6
5	26.8	28.2	11	42.9	44.4	17	22.8	22.6	23	22.8	22.6

| 6 | 26.8 | 28.2 | 12 | 42.9 | 44.4 | 18 | 22.8 | 22.6 | 24 | 22.8 | 22.6 |

Table 6 Comparison of overall redundancy between Model 2 and Model 6

Group number	The removed rods	Rod redundancy order		Overall redundancy *Re*	
		Model 2	Model 6	Model 2	Model 6
1	42	5	1	10.12	44.73
2	41	4	2	11.72	53.31
3	231	17	3	23.44	216.33
4	119	2	4	15.55	60.13
5	215	16	5	31.36	174.16
6	34	20	6	20.35	153.61
7	199	14	7	31.43	175.32
8	110	10	8	21.64	182.24
9	207	1	9	18.70	45.94
10	135	3	10	17.34	14.45

FIGURES

(a) Dalí Museum in St. Petersburg, Florida.   (b) Singapore's Changi Airport

Fig. 1 single-layer grid structures
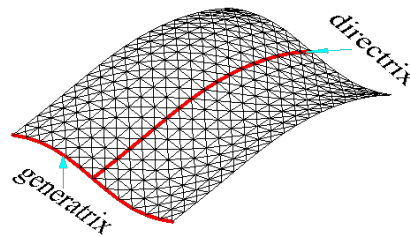
Fig. 2 Shape optimisation of free-form cable-braced grid structure
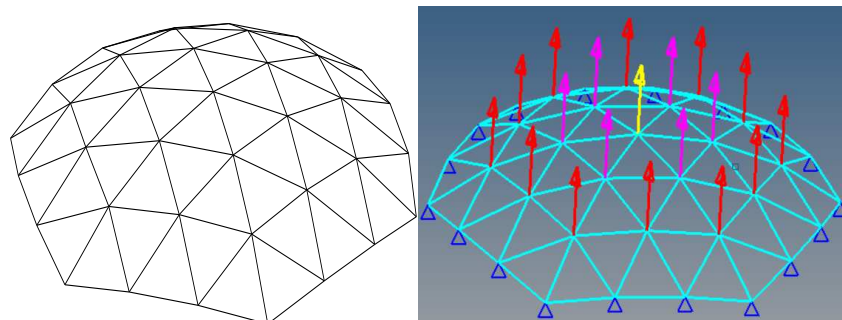
(a) Perspective view   (b) supports and design variables

Fig. 3 Initial model
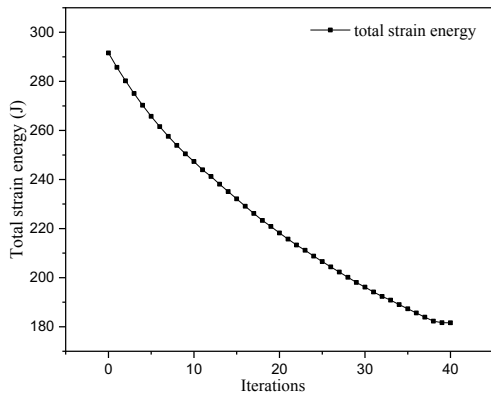
Fig. 4 Variation of total strain energy   Fig. 5 Variation of bending strain energy and its ratio
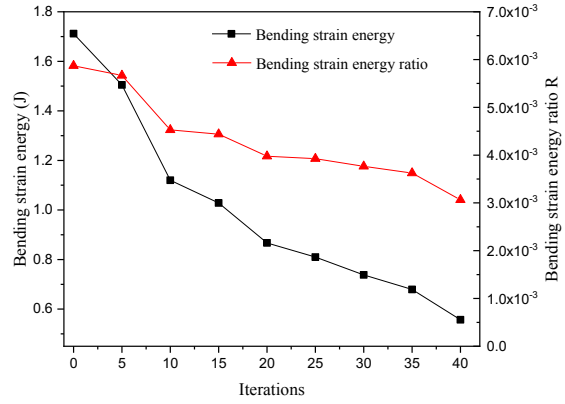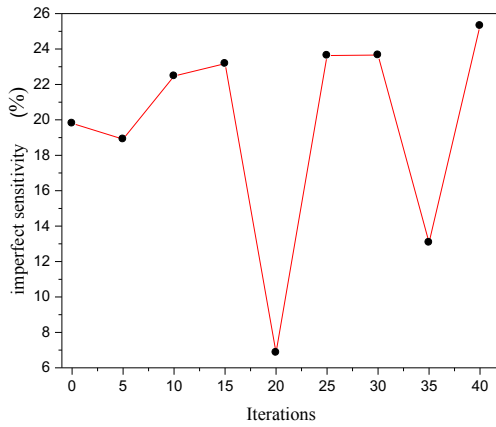
Fig. 6 Fluctuation of imperfection sensitivity   Fig. 7 Variation of buckling load during optimisation
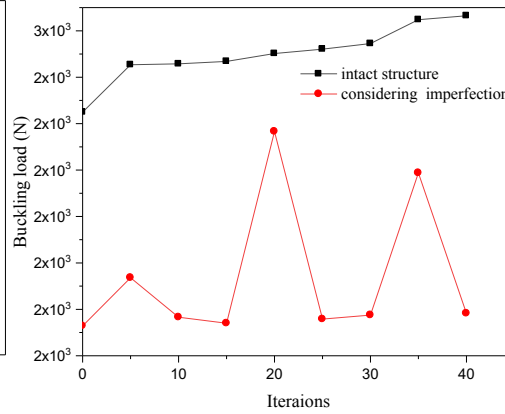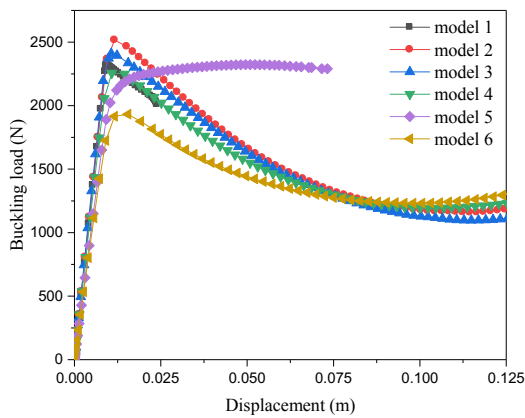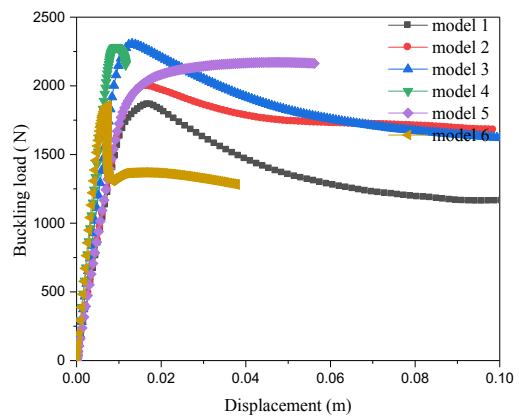
(a) Intact structure   (b) Considering imperfection

Fig. 8 Load-displacement curves of optimised structures
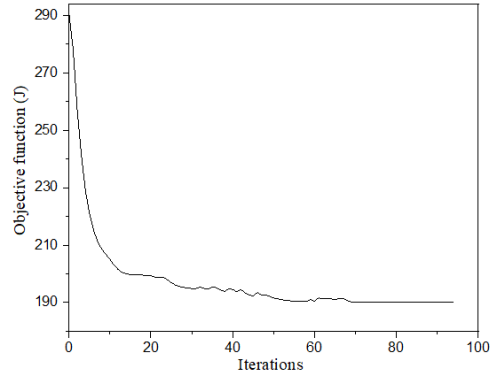
Fig. 9 Iterative curve of model 3

(a) Plan

(b) Perspective
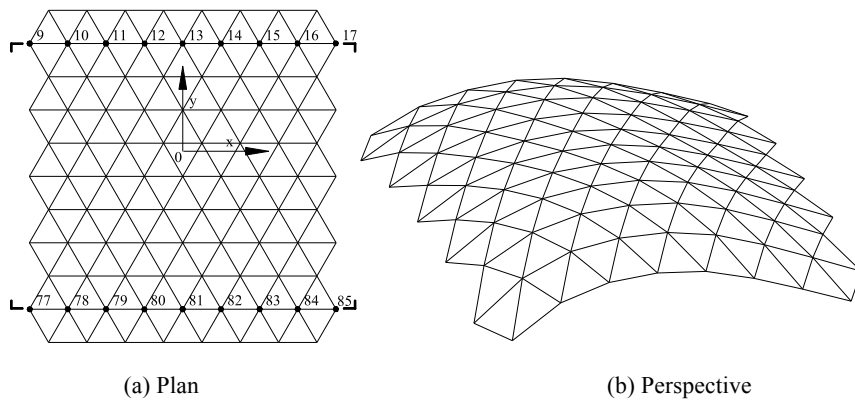
Fig. 10 Structural initial state
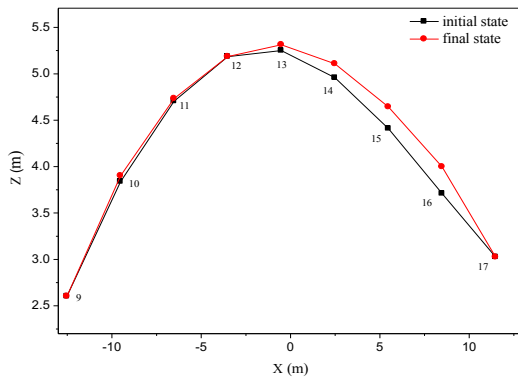
Fig. 11 Coordinate movements of 9-17 nodes
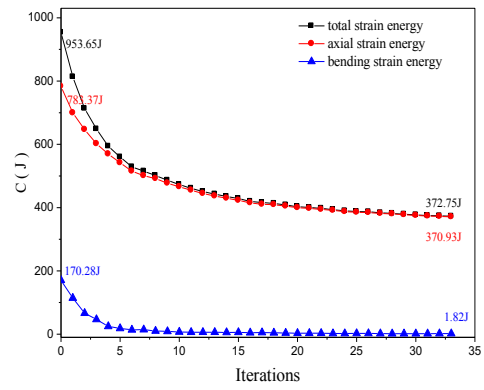
Fig. 12 Variation curves of structural strain energy
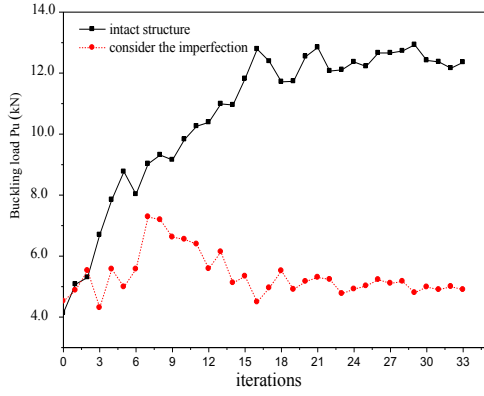
Fig.13 Buckling load variation curves
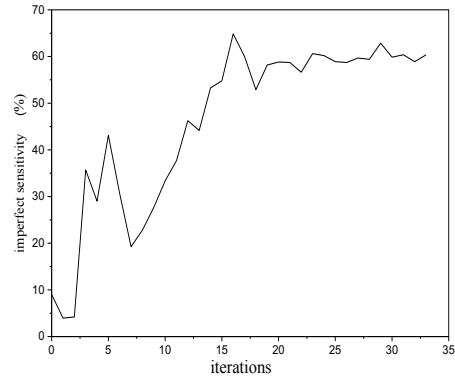
Fig.14 Variation curve of imperfection sensitivity

(a) Model 1and model 2

(b) Model 1and model 3

(c) Model 1and model 4

(d) Model 1and model 5

(e) Model 1and model 6

(f) Model 1and model 7
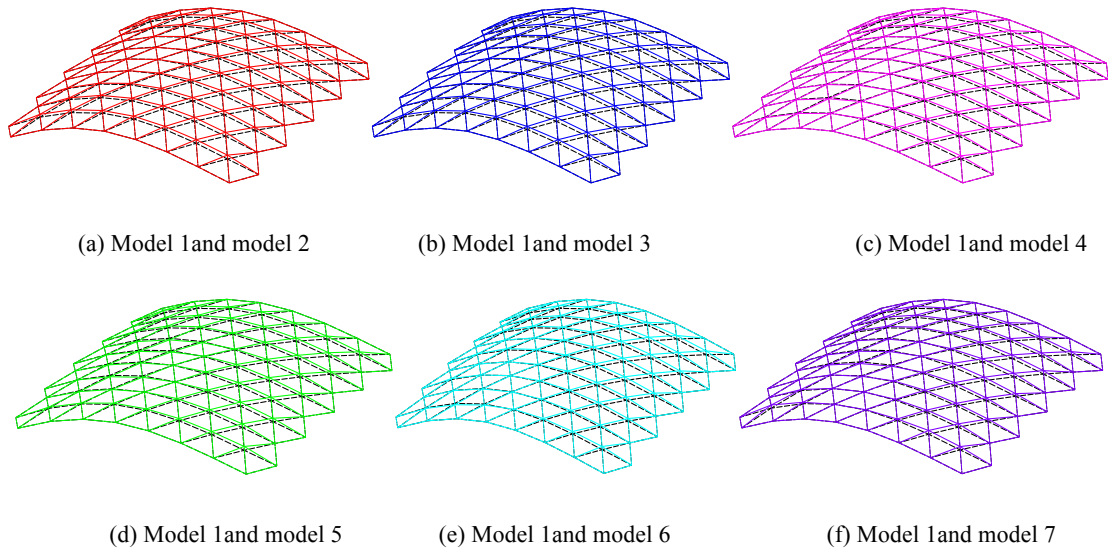
Fig. 15 Shapes after optimisation

(a) Intact structure

(b) Structure considering imperfection
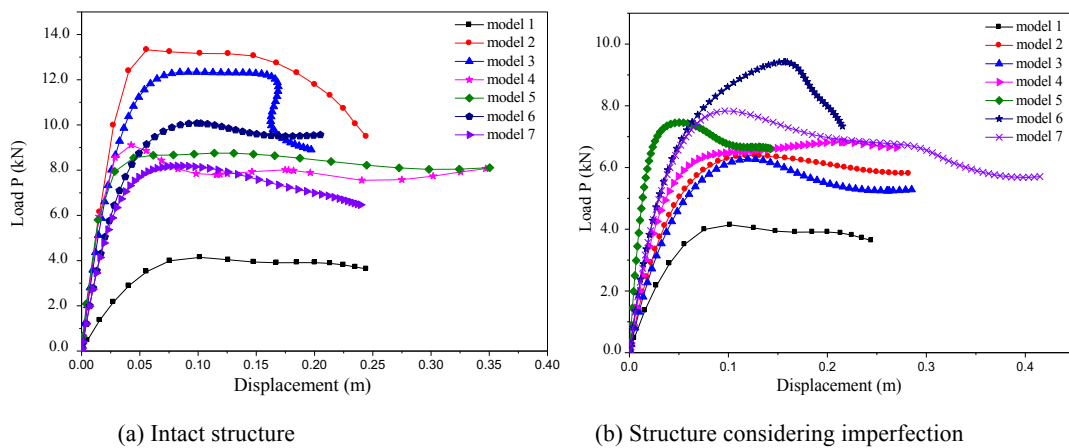
Fig. 16 Load-displacement curves of different models
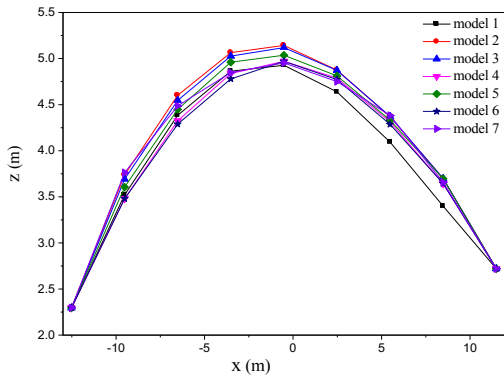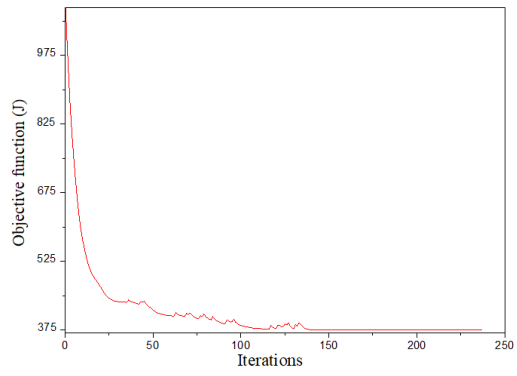
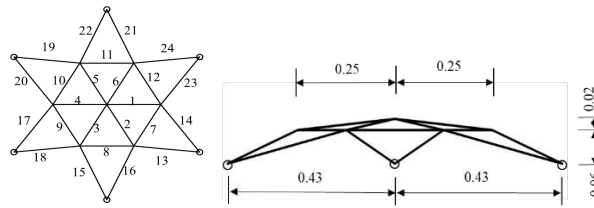Fig. 17 Coordinate changes of nodes 77-85 in each models   Fig. 18 Iterative curve of model 6

(a) Top view   (b) Front view
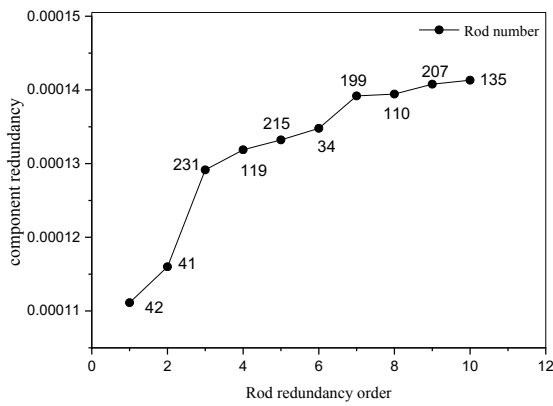
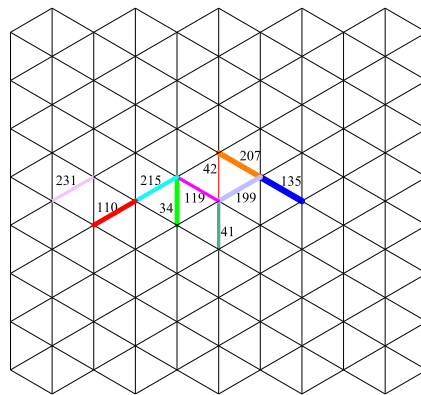Fig. 19 24-member dome (unit: m)

Fig. 20 The first 10 rods with less redundancy in Model 6   Fig. 21 Location of key rods